Title

CRYSTALLOGRAPHY OF THE COMPOUNDS OF CALIFORNIUM. II. CRYSTAL STRUCTURE AND LATTICE PARAMETERS OF CALIFORNIUM OXYCHLORIDE AND CALIFORNIUM SESQUIOXIDE

Authors

Copeland, J.C.
Cunningham, B.B.

Publication Date

1968-06-01

UCRL-18304

cy. 2

University of California

Ernest O. Lawrence Radiation Laboratory

CRYSTALLOGRAPHY OF THE COMPOUNDS OF CALIFORNIUM. II. CRYSTAL STRUCTURE AND LATTICE PARAMETERS OF CALIFORNIUM OXYCHLORIDE AND CALIFORNIUM SESQUIOXIDE

J. C. Copeland and B. B. Cunningham

June 1968

Berkeley, California

DISCLAIMER

To be submitted to
IEEE Transactions on
Instrumentation and Measurements

UCRL-18301
Preprint

UNIVERSITY OF CALIFORNIA

Lawrence Radiation Laboratory
Berkeley, California

AEC Contract No. W-7405-eng-48

ESSENTIAL NONLINEARITY OF PHASE-SENSITIVE DETECTOR CHARACTERISTICS

Branko Leskovar

May 19, 1968

ESSENTIAL NONLINEARITY OF PHASE-SENSITIVE DETECTOR CHARACTERISTICS*

Branko Leskovar

Lawrence Radiation Laboratory
University of California
Berkeley, California

May 19, 1968

ABSTRACT

The effect of essential nonlinearity of phase-sensitive detector characteristics is studied and determined theoretically in detail, assuming that the input signal is a sine wave in the presence of additive narrow-band Gaussian noise. Minimum, maximum, and limiting values of nonlinearities of detector characteristics as functions of the input signal-to-noise ratio and the phase angle between the input signal and the reference wave are determined by means of computer – aided analysis. A set of curves is presented that can be used to evaluate in detail over a wide range of operating conditions and significant parameters the essential nonlinearities of detector performance and characteristics. Particular emphasis is placed on the determination of optimum detector operating conditions for minimum essential nonlinearities in wide-band Fourier-transform high-resolution nuclear magnetic-resonance and electron-spin resonance spectrometers.

I. INTRODUCTION

It has been shown in another paper[1] that the essential nonlinearities of the phase-sensitive detector characteristics result from inherent detector behavior at the amplitude or phase detection of the input signal in the presence of noise. They do not involve nonlinearities resulting from the nonlinearity of characteristics of the electronic components used, or from the unbalance between the channels of the phase-sensitive detector. However, its total nonlinearity from these causes can be kept well below 1% in a wide dynamic range for most applications by (a) employing new and well matched components, (b) careful balancing of the detector channels, and (c) using the double-balanced technique in the design of a phase-sensitive detector. Consequently, essential nonlinearities of detector characteristics have become very important, especially in wide-band phase-sensitive detection used in Fourier-transform high-resolution nuclear magnetic-resonance and electron-spin resonance spectrometers. In these applications the effect of detector nonlinearity must be evaluated, since the shape of the recorded resonance can be altered. Furthermore, essential nonlinearities cannot be reduced by using new components and better matching techniques, but they can be minimized by using proper operating conditions for a particular application.

According to Fig. 1, which is based on the previously mentioned paper, the normalized form of the phase-sensitive characteristics used for determination of detector nonlinearities is given by

$$\frac{V_0}{V_\sigma} = \eta_d \left(\frac{\pi}{2}\right)^{1/2} \left\{ u[v(x)] - y[t(x)] \right\}, \qquad (1)$$

where functions $u[v(x)]$ and $y[t(x)]$ are given by

$$u[v(x)] = {}_1F_1\left(-\frac{1}{2};\ 1;\ -\frac{V_\alpha^2}{2V_\sigma^2}\right), \tag{2}$$

$$y[t(x)] = {}_1F_1\left(-\frac{1}{2};\ 1;\ -\frac{V_\beta^2}{2V_\sigma^2}\right). \tag{3}$$

Terms V_α and V_β are defined by

$$V_\alpha^2 = V_c^2 + V_s^2 + 2V_cV_s\cos\psi, \tag{4}$$

$$V_\beta^2 = V_c^2 + V_s^2 - 2V_cV_s\cos\psi. \tag{5}$$

By using a notation consistent with Ref. 1, V_0 is the detector output signal, V_σ is the root-mean-square value of the input narrow-band noise, η_d is the detection efficiency, V_s is the amplitude of the input sine signal, V_c is the amplitude of the reference wave, ψ is the phase angle between the input signal and the reference wave, and ${}_1F_1$ denotes the confluent hypergeometric function defined by

$$\begin{aligned} {}_1F_1(a;b;\pm p) &= 1 + \frac{a}{b}\cdot\frac{(\pm p)}{1!} + \frac{a(a+1)}{b(b+1)}\cdot\frac{(\pm p)^2}{2!} + \frac{(a)_n}{(b)_n}\cdot\frac{(\pm p)^n}{n!} + \cdots \\ &= \sum_{n=0}^{\infty}\frac{(a)_n}{(b)_n}\cdot\frac{(\pm p)^n}{n!}, \end{aligned} \tag{6}$$

where
$$\begin{aligned} (a)_n &= a(a+1)\cdots(a+n-1), \quad (a)_0 = 1, \\ (b)_n &= b(b+1)\cdots(b+n-1), \quad (b)_0 = 1. \end{aligned} \tag{7}$$

Generally, three important cases of the nonlinearity of the phase-sensitive detector characteristics have been found. In the first case, the detector nonlinearity N_A has been determined as a function of the input signal-to-noise ratio for the phase angle ψ between the input signal and

the reference wave equal to $2n\pi$, where $n = 0, \pm1, \pm2, \cdots$. In the second and the third cases, the detector nonlinearities N_B and N_C have been obtained as a function of the phase angle and the input signal-to-noise ratio. In all cases, nonlinearities N_A, N_B, and N_C have been evaluated from the extent of their departure from the tangent drawn from the characteristic at points $V_s/V_\sigma = 0$, $\psi_2 = (2n+1)\,\pi/2$, and $\psi_1 = 2n\pi$, respectively. Obtained expressions are suitable for a numerical calculation of nonlinearities in different regions of the detector operation, for a general type of push-pull phase-sensitive detector. Application of phase-sensitive detection in contemporary experimental physics instrumentation, electrical measurements, and automatic control systems demands nonlinearity evaluation in detail over a wide range of operating conditions and significant parameters. For example, nonlinearity evaluation is often presently demanded for a range of the input signal-to-noise ratio from 10^{-2} to 10^{4} and the reference wave-to-input noise ratio from 1 to 10^{4} in the wide-band phase-sensitive detection. The purpose of this paper is to calculate minimum, maximum, and limiting values of essential detector nonlinearities N_A, N_B, and N_C, and to evaluate detector performance over a wide range of operating conditions and significant parameters.

II. NONLINEARITY OF DETECTOR CHARACTERISTICS RELATING TO THE INPUT SIGNAL-TO-NOISE RATIO FOR PHASE ANGLE $\psi = 2n\pi$

For this case the essential nonlinearity N_A can be calculated over a wide range of operating conditions according to Ref. 1 by means of the equation

$$N_A = 1 - \frac{1}{x\mu}\,\frac{\gamma[f(x)] - \omega[\epsilon(x)]}{\chi(\mu)}, \tag{8}$$

where

$$x = \frac{V_s}{V_\sigma}, \tag{9}$$

$$\mu = \frac{V_c}{V_\sigma}, \tag{10}$$

$$\gamma[f(x)] = {}_1F_1\left(-\frac{1}{2};\ 1;\ -\frac{V_c^2 + V_s^2}{2V_\sigma^2}\right), \tag{11}$$

$$\omega[\epsilon(x)] = {}_1F_1\left(-\frac{1}{2};\ 1;\ -\frac{V_c^2 - V_s^2}{2V_\sigma^2}\right), \tag{12}$$

$$\chi(\mu) = {}_1F_1\left(\frac{1}{2};\ 2;\ -\frac{V_c^2}{2V_\sigma^2}\right). \tag{13}$$

Since the expression for nonlinearity N_A has been derived for $\psi = 2n\pi$, N_A depends only on the input signal-to-noise ratio V_s/V_σ and the reference wave-to-noise V_c/V_σ.

By means of a digital computer, the nonlinearity N_A as a function of the input signal-to-noise ratio with the reference wave-to-noise ratio as parameter is calculated and plotted as shown in Fig. 2. High accuracy numerical calculations of the confluent hypergeometric function in Eq. (8) are performed in two different ways. Where the variable of the hypergeometric function is smaller than 20, the function is expressed and calculated in terms of the modified Bessel functions of the first kind according to the relations[2]

$${}_1F_1\left(-\frac{1}{2};\ 1;\ -p\right) = \exp\left(-\frac{p}{2}\right)\left[(1+p)I_0\left(\frac{p}{2}\right) + x\,I_1\left(\frac{p}{2}\right)\right] \tag{14a}$$

$${}_1F_1\left(\frac{1}{2};\ 2;\ -p\right) = \exp\left(-\frac{p}{2}\right)\left[I_0\left(\frac{p}{2}\right) + I_1\left(\frac{p}{2}\right)\right]. \tag{14b}$$

For the hypergeometric function variable larger than 20, asymptotic expansion according to the following formula[3] is used:

$$
{}_1F_1(a;b;p) = \frac{\Gamma(b)}{\Gamma(b-a)}\left[\frac{\exp(i\pi\tau)}{p}\right]^a \sum_{n=0}^{M} \frac{(a)_n (a-b+1)_n}{n!\,(-p)^n}
$$

$$
+ O\left(|p|^{-a-M-1}\right) + \frac{\Gamma(b)}{\Gamma(a)} \exp(p)\cdot p^{a-b} \sum_{n=0}^{N} \frac{(b-a)_n (1-a)_n}{n!\,p^n} \qquad (15)
$$

$$
+ O\left(|\exp(p)\cdot p^{a-b-N-1}|\right),
$$

where $\Gamma(b)$, $\Gamma(b-a)$, $\Gamma(a)$ denote the gamma functions $M, N = 0, 1, 2, \cdots$, $\tau = 1$ if $\mathrm{Im}\,p > 0$, $\tau = -1$ if $\mathrm{Im}\,p < 0$, $-\pi < \arg p < \pi$; $O(|p|^{-a-M-1})$ and $O(|\exp(p)\,p^{a-b-N-1}|)$ denote the order of magnitude of $|p|^{-a-M-1}$ and $|\exp(p)\cdot p^{a-b-N-1}|$, respectively.

In particular if $M \to \infty$, $N \to \infty$ the asymptotic relation becomes

$$
{}_1F_1(a;b;-p) \sim \frac{\Gamma(b)}{\Gamma(b-a)} p^{-a} \sum_{n=0}^{\infty} \frac{(a)_n (a-b+1)_n}{n!\,p^n} = \frac{\Gamma(b)}{\Gamma(b-a)} p^{-a}\left[1 + \frac{a(1+a-b)}{1!\,p}\right.
$$

$$
\left. + \frac{a(a+1)(1+a-b)(2+a-b)}{2!\,p^2} + \frac{a(a+1)(a+2)(1+a-b)(2+a-b)(3+a-b)}{3!\,p^3} + \cdots\right], \qquad (16)
$$

where $\mathrm{Re}\,p > 0$, $(a)_n$ is defined by Eq. (7), and

$$
(a-b+1)_n = (1+a-b)(2+a-b)\cdots(n+a-b);\ (a-b+1)_0 = 1. \qquad (17)
$$

Taking $a = -1/2$; $b = 1$, and $a = 1/2$; $b = 2$, the hypergeometric functions in Eq. (6) will be asymptotically equal:

$$
{}_1F_1\left(-\frac{1}{2};\ 1;\ -p\right) \sim 2\left(\frac{p}{\pi}\right)^{1/2}\left(1 + \frac{1}{1!4p} + \frac{1}{2!16p^2} + \frac{9}{3!64p^3} + \frac{225}{4!256p^4} + \cdots\right), \qquad (18)
$$

$$ {}_1F_1\left(\frac{1}{2};\, 2;\, -p\right) \sim 2\left(\frac{1}{\pi p}\right)^{1/2} \left(1 - \frac{1}{1!\,4p} - \frac{3}{2!\,16p^2} - \frac{45}{3!\,64p^3} - \cdots\right). \quad (19) $$

The error is approximately equal to 10^{-7} if 5 terms are used on the right-hand side of formula (16) and 2.10^{-6} if 4 terms are used in (17), for $p \geq 20$. The total error of the calculated nonlinearity values N_A has been approximately equal to 5.10^{-7} by using the expression (6) and the first 8 terms on the right-hand side of both equations(18) and (19) including computer limitations.

Curves in Fig. 2 show that the nonlinearity N_A can be considerably decreased by increasing the reference wave-to-input noise ratio to the signal-to-noise ratio. For example, an increase of the reference wave-to-noise ratio to the signal-to-noise ratio for one order of magnitude will decrease the nonlinearity for three orders of magnitude, for $V_s/V_\sigma = 1$. Furthermore, the nonlinearity will be even more reduced for larger amounts of the signal-to-noise ratio. It can be seen that for $V_c/V_\sigma = 10$ an increase of V_c/V_σ by one order of magnitude will decrease the nonlinearity more than four orders of magnitude. Consequently, the gain in the nonlinearity decreasing will be larger for larger amounts of the input signal-to-noise ratio, for the same increase of the reference wave-to-noise ratio to the signal-to-noise ratio. However, for purposes of obtaining the largest output signal and a wide dynamic range in the wide-band phase-sensitive detection application by using solid-state components, the input signal-to-noise ratio is close in value to the reference wave-to-noise ratio. In such applications the essential nonlinearity can have an appreciable value, especially for small amounts of V_c/V_σ and V_s/V_σ. With increasing V_c/V_σ and V_s/V_σ ratios the essential nonlinearity will be gradually decreased, as

can be concluded by a comparison of the curves given in Fig. 2. For the case $V_c/V_\sigma = V_s/V_\sigma$, the following approximation values of the nonlinearity N_A can be seen from Fig. 2: 8.5, 5.2, 0.51, and 0.035% for V_s/V_σ equals 1, 10, 10^2, and 10^3, respectively. However, for cases where both V_c/V_σ and V_s/V_σ have amounts larger than 10, the reference wave-to-noise ratio always has to be slightly larger than the input signal-to-noise ratio. If this condition is not satisfied the nonlinearity can reach an unacceptably high value; e.g., for $V_c/V_\sigma = 100$ and $V_c/V_\sigma = 80$ the nonlinearity will be approximately equal to 0.01%. On the other hand for $V_c/V_\sigma = 100$ and $V_s/V_\sigma = 120$, nonlinearity will be more than three orders of magnitude larger, approximately more than 10%. This amount is unacceptable for most practical applications. Generally, the nonlinearity deterioration will be larger for larger values of both V_c/V_σ and V_s/V_σ under previously mentioned conditions. Consequently, wherever the essential nonlinearity is of a prime importance, the maximum signal-to-noise ratio value should be always smaller than the reference wave-to-noise ratio value, irrespective of other demands which can be imposed on the phase-sensitive detection system for other reasons. This is particularly important in applications where the input signal-to-noise ratio varies in a wide dynamic range. If the signal-to-noise ratio is only 10% smaller than the reference wave-to-noise ratio, the nonlinearity N_A can be reduced for more than one and a half orders of magnitude, which can be concluded by an inspection and comparison of curves for $V_c/V_\sigma = 10^2$, 10^3 and 10^4 in Fig. 2.

III. NONLINEARITIES OF DETECTOR CHARACTERISTICS RELATING TO THE PHASE ANGLE BETWEEN THE INPUT SIGNAL AND THE REFERENCE WAVE

The essential nonlinearities N_B and N_C of the detector characteristics with respect to the phase angle between the input signal and the reference wave can be determined over a wide range of operating conditions according to Ref. 1 by expressions

$$N_B = 1 - \frac{1}{x\mu} \frac{u[v(x)] - y[t(x)]}{w[f(x)]\left(\frac{\pi}{2} - \psi\right)} \tag{20}$$

and

$$N_C = 1 - \frac{u[v(x)] - y[t(x)]}{\phi[g(x)] - z[h(x)]}, \tag{21}$$

where $x = V_s/V_\sigma$, $\mu = V_c/V_\sigma$. Other functions are defined by relations (2) and (3) and by the following expressions:

$$w[f(x)] = {}_1F_1\left(\frac{1}{2}; 2; -\frac{V_c^2 + V_s^2}{2V_\sigma^2}\right), \tag{22}$$

$$\phi[g(x)] = {}_1F_1\left[-\frac{1}{2}; 1; -\frac{(V_c + V_s)^2}{2V_\sigma^2}\right], \tag{23}$$

$$z[h(x)] = {}_1F_1\left[-\frac{1}{2}; 1; -\frac{(V_c - V_s)^2}{2V_\sigma^2}\right]. \tag{24}$$

Nonlinearities N_B and N_C have been calculated in relation to the phase characteristic operating points $\psi_2 = (2n+1)\,\pi/2$ and $\psi_1 = 2n\pi$, respectively. Both nonlinearities depend upon the phase angle, the input signal-to-noise ratio, and the reference wave-to-noise ratio. By using

equations from (20) to (24), nonlinearities N_B and N_C are numerically calculated and shown in Fig. 3. The signal-to-noise and the reference wave-to-noise ratios of 1, 10^2, 10^3, and 10^4 are chosen as parameters.

The curves in the figure show that for $V_c/V_\sigma = V_s/V_\sigma = 1$, the nonlinearity N_B will be smaller than 1% if the phase-angle deviation is $\Delta\psi \leq 0.95\ \pi/12$. The phase-angle deviation can be $\Delta\psi \leq 1.76\ \pi/12$ for the same nonlinearity value if $V_c/V_\sigma = V_s/V_\sigma \geq 10$. The maximum nonlinearity $N_{B,\,max}$ appears at the point $\psi_1 = 2n\pi$, but its value depends on the input signal-to-noise and the reference wave-to-noise ratios. For the case $V_c/V_\sigma = V_s/V_\sigma$, the following maximum nonlinearities $N_{B,\,max}$ can be calculated from Eq. (20): 35.41, 15.28, 10.52, 10.02, and 9.97% for the signal-to-noise ratios 1, 10, 10^2, 10^3, and 10^4. Generally, the maximum nonlinearity will be smaller for a larger amount of V_c/V_σ and V_s/V_σ. However, to obtain a better insight about nonlinearity behavior with the signal-to-noise ratio variation, the nonlinearity N_B is calculated and plotted in Figs. 4 and 5 with the following fixed values of V_c/V_σ: 1, 10^2, 10^3, and 10^4, and ψ: 0, $\pi/6$, $\pi/4$, $\pi/3$, $5\pi/12$, $11\pi/24$, $47\pi/96$, and $99\pi/200$.

For this purpose, relative minimums of functions (20) with respect to $x = V_s/V_\sigma$, using $\mu = V_c/V_\sigma$ and ψ as parameters, are also calculated. The nonlinearity relative minimum is determined by the differential calculus standard procedure by using the partial differentiation with respect to V_s/V_σ and equalizing it to zero.

$$\frac{\partial}{\partial x}(N_B) = \frac{\partial}{\partial x}\left\{-\frac{u[v(x)]}{x\mu\left(\frac{\pi}{2}-\psi\right)\,w[f(x)]}\right\} + \frac{\partial}{\partial x}\left\{\frac{y\,t(x)}{x\mu\left(\frac{\pi}{2}-\psi\right)\,w[f(x)]}\right\} = 0. \qquad (25)$$

Using the expression for the confluent hypergeometric function derivative,

$$\frac{d^n}{d_p^n}\left[{}_1F_1\,(a;b;p)\right] = \frac{(a)_n}{(b)_n}\,{}_1F_1\,(a+n;\,b+n;\,p). \tag{26}$$

Differentiation and the equalization of (25) to zero give the result

$$w[f(x)]\left\{\left(\frac{x^2}{2}+\frac{\mu\cos\psi}{2}\,x\right)s[v(x)]-\left(\frac{x^2}{2}-\frac{\mu\cos\psi}{2}\,x\right)m[t(x)]+y[t(x)]-u[v(x)]\right\}$$

$$-\left(\frac{x}{2}\right)^2 K[f(x)]\left\{y[t(x)]-u[v(x)]\right\}=0, \tag{27}$$

where $w[f(x)]$, $y[t(x)]$, $u[v(x)]$ are given by relations (22), (3), (2), respectively. The other functions are defined by:

$$s[v(s)] = {}_1F_1\left(\frac{1}{2};\,2;\,-\frac{V_\alpha^{\,2}}{2V_\sigma^{\,2}}\right), \tag{28}$$

$$m[t(x)] = {}_1F_1\left(\frac{1}{2};\,2;\,-\frac{V_\beta^{\,2}}{2V_\sigma^{\,2}}\right), \tag{29}$$

$$K[f(x)] = {}_1F_1\left(\frac{3}{2};\,3;\,-\frac{V_c^{\,2}+V_s^{\,2}}{2V_\sigma^{\,2}}\right). \tag{30}$$

From curves in Fig. 4 it can be seen that for $V_c/V_\sigma = 1$ the nonlinearity N_B will be practically independent of the input signal-to-noise ratio. Curves have a small minimum at point $V_s/V_\sigma = 2.482$. However, the nonlinearity strong dependence upon the phase angle is readily evident. Furthermore, for $V_c/V_\sigma \geq 10$ the nonlinearity minimum value $N_{B,\,min}$

strongly depends upon V_c/V_σ and V_s/V_σ ratios, as well as on phase angle ψ. For any phase angle value, the detector characteristics will have an nonlinearity minimum amount if V_c/V_σ is close in amount to V_s/V_σ. Approximate values of the minimum nonlinearity input signal-to-noise ratio can be found from the transcendental equation (27) for any amount of V_c/V_σ and ψ by a numerical method. The minimum nonlinearity $N_{B,\,min}$ is approximately a half order of magnitude smaller than its average value for almost any value of ψ. Generally, the mininum nonlinearity will be smaller for larger signal-to-noise and reference wave-to-noise ratios. In addition, the limit of nonlinearity N_B as ψ tends to $(2n+1)\,\pi/2$ is zero, which we write as

$$\lim_{\psi \to (2n+1)\frac{\pi}{2}} N_B = 0. \tag{31}$$

Figure 3 also illustrates the behavior of nonlinearity N_C for $V_c/V_\sigma = V_s/V_\sigma = 1,\ 10,\ 10^2,\ 10^3$, and 10^4. Nonlinearity N_C will be smaller than 1% if the phase angle deviation $\Delta\psi \leq 0.53\,\pi/12$, for $V_s/V_\sigma = V_c/V_\sigma = 1$. The phase angle deviation can be $\Delta\psi \leq 0.28\,\pi/12$ for the same nonlinearity value if $V_c/V_\sigma = V_s/V_\sigma \geq 10$. The maximum nonlinearity N_C for any value of V_c/V_σ and V_s/V_σ appears at point $\psi_2 = (2n+1)\pi/2$ and its limit is

$$\lim_{\psi \to (2n+1)\frac{\pi}{2}} N_C = 1. \tag{32}$$

Furthermore, for obtaining the optimum detector operating conditions, the nonlinearity N_C is calculated and plotted in Figs. 6 and 7 for the following values of V_c/V_σ: 1, 10, 10^2, 10^3, and 10^4; and ψ: $47\pi/96$, $\pi/3$,

$\pi/4$, $\pi/12$, $\pi/24$, $\pi/48$, $\pi/96$, and $\pi/300$.

In addition to the above, the relative maximum of functions (21) with respect to $x = V_s/V_\sigma$ with $\mu = V_c/V_\sigma$ and ψ as parameters are also calculated. The nonlinearity relative maximum is obtained by using the function partial differentiation with respect to V_s/V_σ and equalizing it to zero:

$$\frac{\partial}{\partial x}(N_C) = \frac{\partial}{\partial x}\left\{-\frac{u[v(x)]}{\phi[g(x)] - z[h(x)]}\right\} + \frac{\partial}{\partial x}\left\{\frac{y[t(x)]}{\phi[g(x)] - z[h(x)]}\right\} = 0. \tag{33}$$

By using relation (26), differentiation and equalization to zero give

$$\left\{\phi[g(x)] - z[h(x)]\right\}\left\{\left(\frac{x}{2} - \frac{\mu}{2}\cos\psi\right) m[t(x)] - \left(\frac{x}{2} + \frac{\mu}{2}\cos\psi\right) s[v(x)]\right\}$$
$$+ \left\{\left(\frac{x}{2} + \frac{\mu}{2}\right)\rho[g(x)] - \left(\frac{x}{2} - \frac{\mu}{2}\right)\ell[h(x)]\right\}\left\{u[v(x)] - y[t(x)]\right\} = 0, \tag{34}$$

where $u[v(x)]$, $y[t(x)]$, $\phi[g(x)]$, $z[h(x)]$, $s[v(x)]$, and $m[t(x)]$ are given by relations (2), (3), (23), (24), (28), and (29), respectively. Other functions are defined by

$$\rho[g(x)] = {}_1F_1\left[\frac{1}{2};\ 2;\ -\frac{(V_c + V_s)^2}{2V_\sigma^2}\right], \tag{35}$$

$$\ell[h(x)] = {}_1F_1\left[\frac{1}{2};\ 2;\ -\frac{(V_c - V_s)^2}{2V_\sigma^2}\right]. \tag{36}$$

From curves in Figs 5 and 6 it follows that nonlinearity N_C will be almost independent on the signal-to-noise ratio for $V_c/V_\sigma = 1$. For any value of ψ, curves have a maximum for $V_s/V_\sigma = 2.536$. The nonlinearity will strongly depend on the phase angle for any values of V_c/V_σ

and V_s/V_σ as well as upon the signal-to-noise ratio if $V_c/V_\sigma \geq 10$. Generally, in these cases, the nonlinearity N_C will have a maximum value for a given ψ, if both ratios V_c/V_σ and V_s/V_σ are approximately equal. A numerical solution of transcendental equation (34) gives the input signal-to-noise ratio amount of the maximum nonlinearity $N_{C,max}$. It is approximately one to two orders of magnitude larger than its average value for any value of ψ. The maximum nonlinearity will be larger for larger values of both V_c/V_σ and V_s/V_σ and for smaller values of ψ in comparison with its average value.

Finally, the limit of N_C as ψ tends to $2n\pi$ is zero, or

$$\lim_{\psi \to 2n\pi} N_C = 0. \tag{37}$$

CONCLUSIONS AND COMPARISONS

The theoretical minimum, maximum, and limiting values of the nonlinearities of detector characteristics are expressible over a wide dynamic range of operating conditions in terms of well-known functions. Obtained expressions and curves in Fig. 2 illustrate the behavior of essential nonlinearities N_A of characteristics of a phase-sensitive detector which used idealized linear electric components. The curves of Fig. 2 show that for a fixed phase angle ψ, the proper choice of V_c/V_σ and V_s/V_σ will minimize the characteristic nonlinearity N_A to an acceptable amount. This is particularly important in wide-frequency band and wide dynamic range phase-sensitive detection applications where V_c/V_σ is often close in value to V_s/V_σ, resulting in a large essential

nonlinearity. Furthermore, a comparison of expressions (20) and (21) and curves for N_B and N_C in Fig. 3 shows that the nonlinearity N_B is smaller than the nonlinearity N_C for the same phase angle deviation $\Delta\psi$ around the operating point. In addition to the above curves (N_B and N_C versus ψ for constant V_s/V_σ), another set of curves in Figs. 4 and 5 show N_B and N_C versus V_s/V_σ for constant V_c/V_σ and ψ. The curves of Figs 4 and 5 show that for a fixed V_c/V_σ and ψ, the proper choice of V_s/V_σ will minimize the nonlinearity N_B. The best value of the input signal-to-noise ratio can be found by solution of transcendental equation (27). For $\psi = \pi/4$ and $V_c/V_\sigma = 1$, 10, 10^2, 10^3, and 10^4, the nonlinearity N_B is minimized for $V_s/V_\sigma = 2.48274$, 1.00935, 1.00004, 1.00000, and 1.00000, respectively. Any other V_s/V_σ value can be considered as a nonoptimum one, although the nonlinearity increase will not be significant for $V_c/V_\sigma = 1$ and for the small amounts of ψ. Furthermore, the proper value of V_s/V_σ will also minimize the nonlinearity N_C, which can be concluded from Figs. 6 and 7. For this purpose it is important to avoid the region where curve N_C versus V_s/V_σ has a maximum. This particularly nonoptimum V_s/V_σ value can be found for any V_s/V_σ ratio and ψ by numerical solution of Eq. (34). If $\psi = \pi/24$ and $V_c/V_\sigma = 1$, 10, 10^2, 10^3, and 10^4, the nonlinearity N_C is maximized for $V_s/V_\sigma =$ 2.53699, 1.01915, 1.00010, 1.00000, and 1.00000, respectively. From comparison of N_B and N_C curves it can be seen that nonoptimum values of V_s/V_σ will have far larger influence on the nonlinearity N_C than on the nonlinearity N_B behavior. As such, the nonoptimum V_s/V_σ values maximally increase the N_B for approximately a half order of magnitude in the worst case. However, N_C nonoptimum V_s/V_σ values increase N_C

for two orders of magnitude in the worst case. Consequently, one should choose, whenever possible, the phase angle $\psi_2 = (2n+1)\pi/2$, as an operating point. In this case the larger permissible phase deviation for the same nonlinearity, and the significantly smaller nonlinearity for nonoptimum signal-to-noise ratio will result in comparison with operating point $\psi_1 = 2n\pi$ (case of N_C).

These conclusions and all of the above results are of course based on the assumption that the additive noise in the reference channel may be neglected; the inclusion of additive reference noise in the analysis appears possible, and it would modify these results for a sufficiently strong reference channel noise.

ACKNOWLEDGMENT

The author would like to thank E. Coleman for computer programming.

FOOTNOTE AND REFERENCES

*Work done under the auspices of the U. S. Atomic Energy Commission.

1. B. Leskovar, Phase-Sensitive Detector Nonlinearity at the Signal Detection in the Presence of Noise, IEEE Transactions on Instrumentation and Measurement, Vol. IM-16, No. 4, pp. 285-294, 1967.

2. D. Middleton, An Introduction to Statistical Communication Theory (McGraw-Hill Book Company, Inc., New York, 1960), pp. 1075-1076.

3. A. Erdélyi, W. Magnus, F. Oberhettinger, F. G. Tricomi, Higher Transcendental Functions, Vol. 1 (McGraw-Hill Book Company, Inc., New York, 1953), pp. 277-282.

FIGURE CAPTIONS

Fig. 1. Phase-sensitive detector.

Fig. 2. Behavior of the nonlinearity N_A for the phase angle $\psi = 2n\pi$.

Fig. 3. Comparison of nonlinearities N_B and N_C.

Fig. 4. Nonlinearity N_B as a function of the input signal-to-noise ratio with the phase angle as parameter and the reference wave-to-input noise ratio $V_c/V_\sigma = 1, 10$.

Fig. 5. Nonlinearity N_B as a function of the input signal-to-noise ratio with the phase angle ψ as parameter and the reference wave-to-input noise ratio $V_c/V_\sigma = 10^2, 10^3, 10^4$.

Fig. 6. Nonlinearity N_C as a function of the input signal-to-noise ratio with the phase angle ψ as parameter and the reference wave-to-input noise ratio $V_c/V_\sigma = 1, 10$.

Fig. 7. Nonlinearity N_C as a function of the input signal-to-noise ratio with the phase angle ψ as parameter and the reference wave-to-input noise ratio $V_c/V_\sigma = 10^2, 10^3, 10^4$.

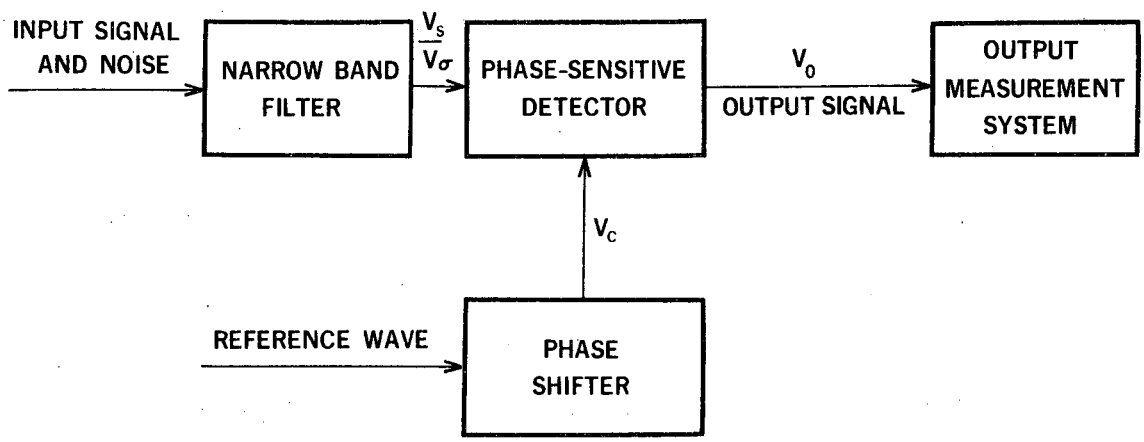

XBL 687-1177

Fig. 1

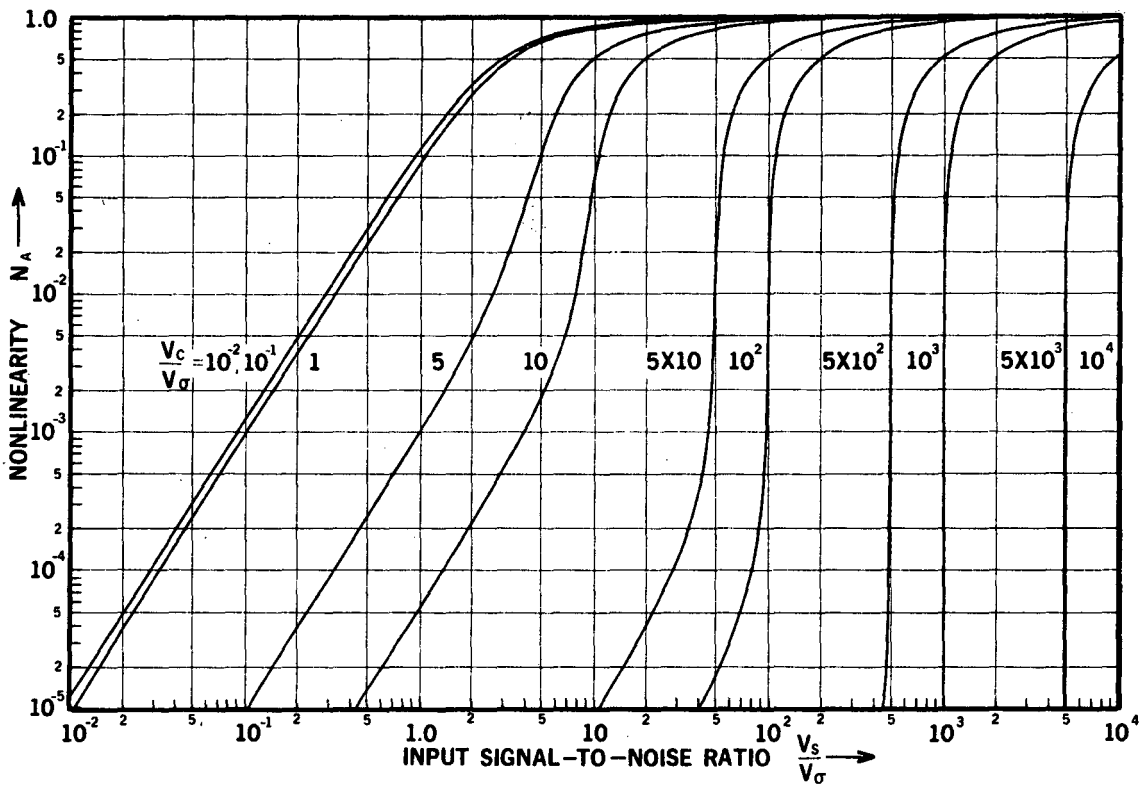

XBL 687-1178

Fig. 2

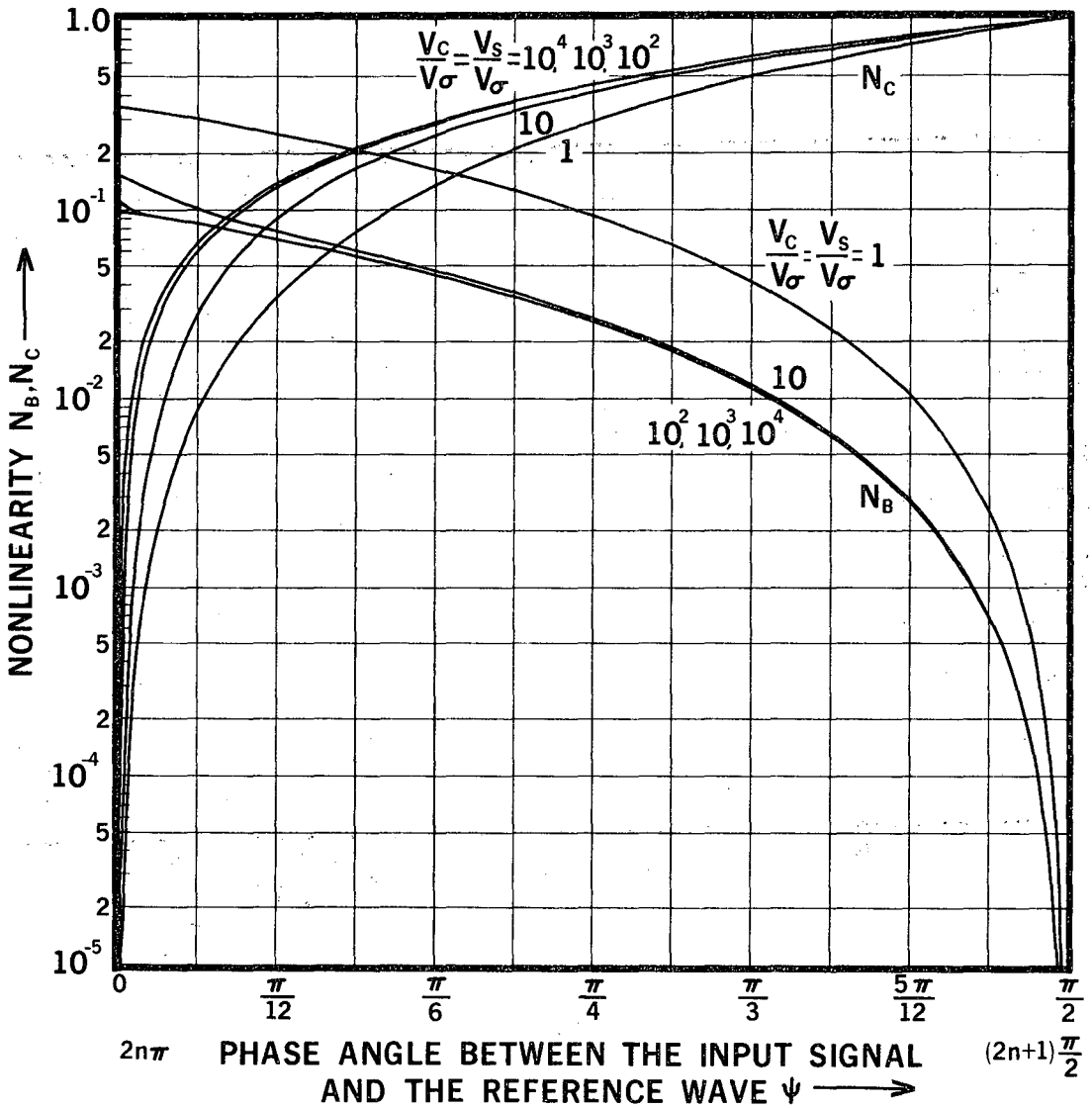

XBL 687-1179

Fig. 3

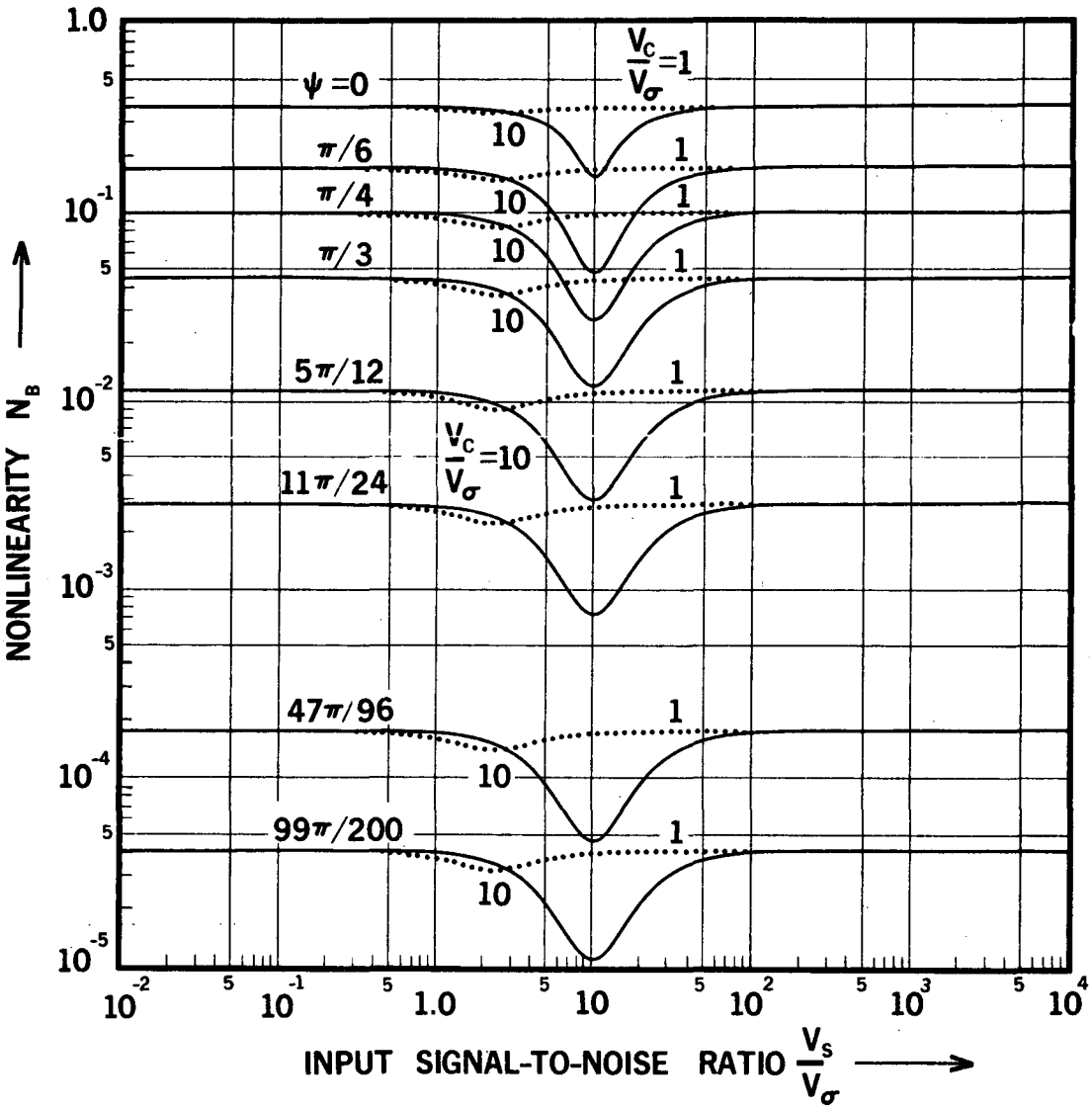

XBL 687-1180

Fig. 4

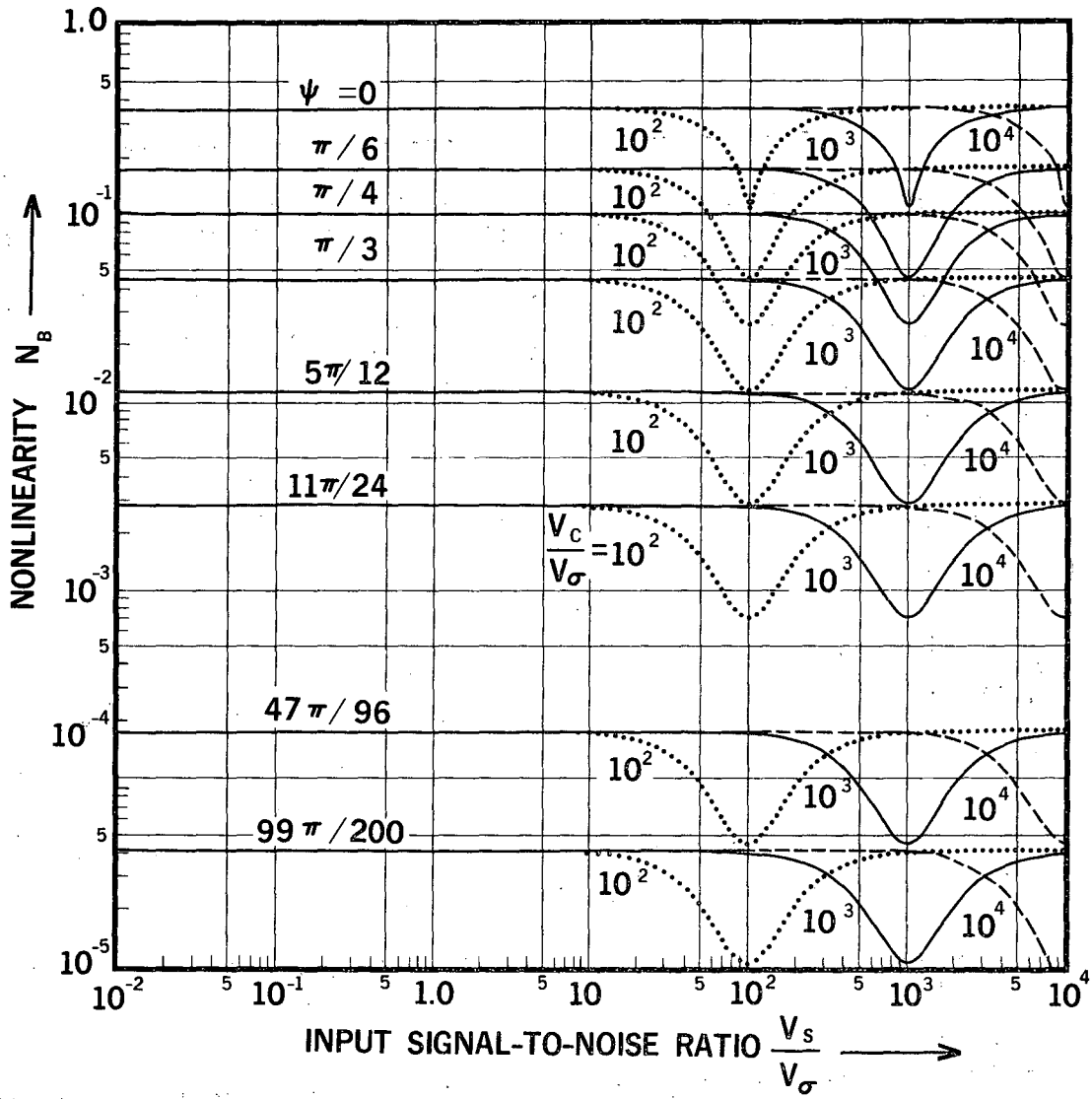

XBL 687-1181

Fig. 5

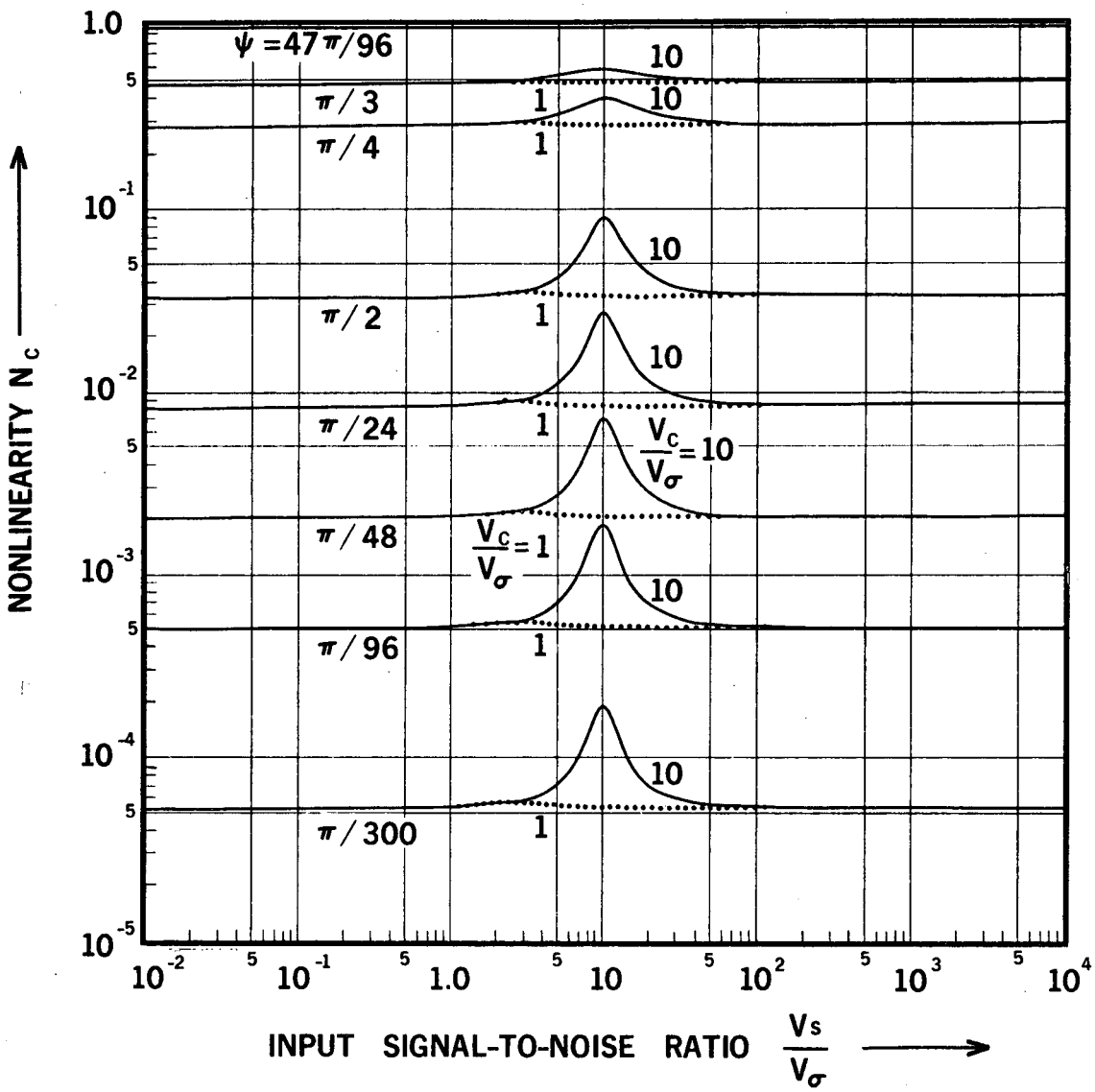

XBL 687-1182

Fig. 6

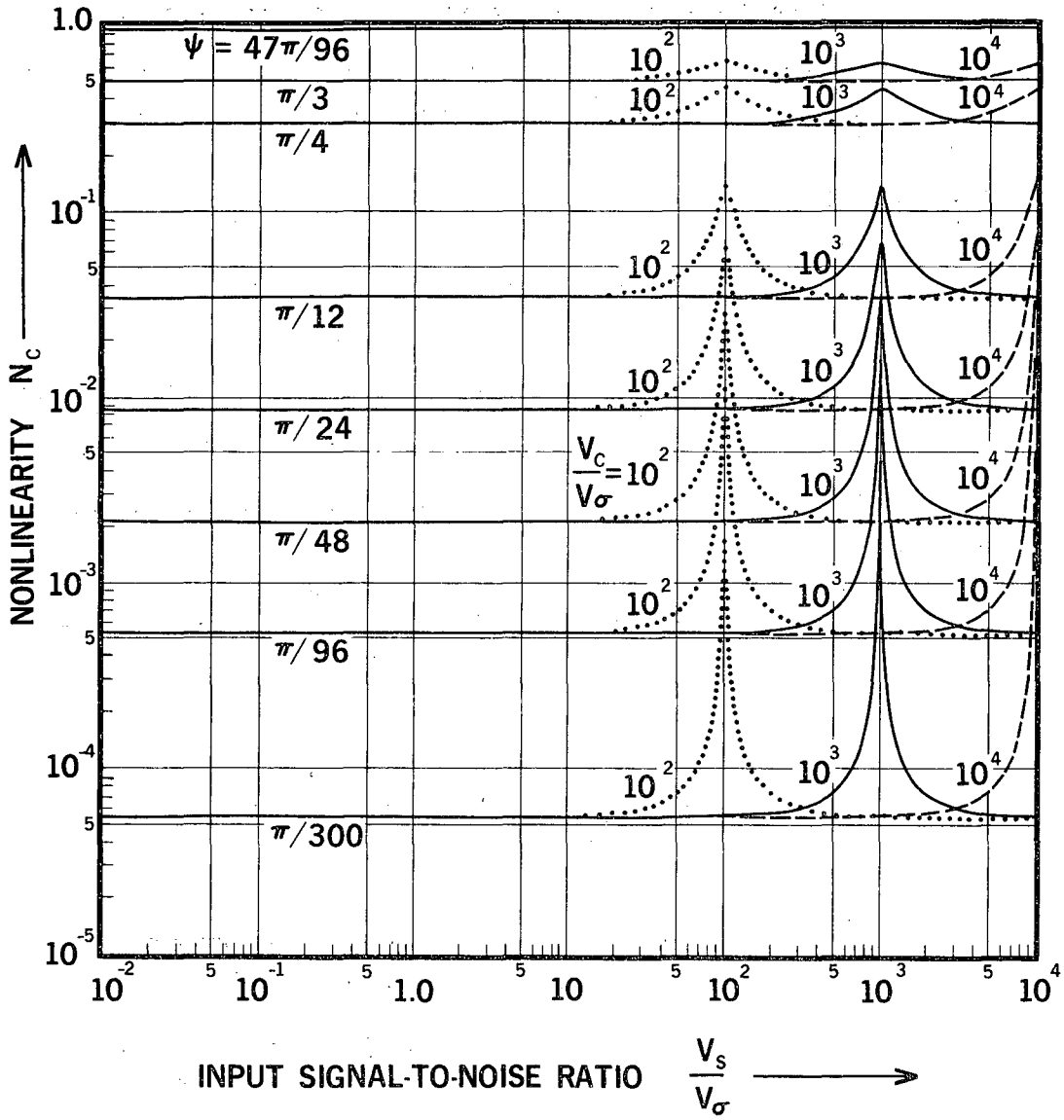

XBL 687-1183

Fig. 7